

We are IntechOpen, the world's leading publisher of Open Access books Built by scientists, for scientists

7,000

Open access books available

186,000

International authors and editors

200M

Downloads

Our authors are among the

154

Countries delivered to

TOP 1%

most cited scientists

12.2%

Contributors from top 500 universities



WEB OF SCIENCE™

Selection of our books indexed in the Book Citation Index
in Web of Science™ Core Collection (BKCI)

Interested in publishing with us?
Contact book.department@intechopen.com

Numbers displayed above are based on latest data collected.
For more information visit www.intechopen.com



High-Gain Amplifier Module Integrating a Waveguide into the Module Case for Millimeter Wave Applications

Young Chul Lee

Additional information is available at the end of the chapter

<http://dx.doi.org/10.5772/intechopen.76622>

Abstract

A high-gain amplifier module with integrated waveguide (WG) has been presented for millimeter wave applications. In order to improve the isolation between the amplification stages in the multi-stage amplifier module, an isolated WG is integrated into the module case. It is possible to effectively suppress the oscillation occurring in the high gain stage. Microstrip line (MSL)-to-WG transitions are designed and fabricated on a 5 mil thick RT5880 substrate for interconnection of the isolated WG, input/output WG and amplifier PCB in a cascaded two-stage high gain amplifier module. The transition loss of -0.44 dB is obtained at 40 GHz and return-loss (S_{11}) bandwidth below -10 dB is from 34.1 to 50 GHz. The fabricated high-gain amplifier module shows a high gain over 39.7 dB from 38 to 41 GHz. At 38.7 GHz, its maximum gain of 44.25 dB is achieved.

Keywords: waveguide, isolation, microstrip-to-waveguide transition, amplifier module

1. Introduction

Recently, millimeter-wave (mm-wave) frequency bands have attracted attention as various applications such as radar sensors [1–3] as well as wireless communication. In particular, due to very widely available bandwidth, frequency bands for a variety of wireless communication applications such as point-to-point wireless communications, radio-on-fiber (RoF) links [4], 5G cellular wireless networks [5], etc. are shifting to the mm-wave frequency band.

One of the key issues for the commercialization of mm-wave systems is reproducible and inexpensive packaging technology in addition to active integrated circuit (IC) technology.

Typically, active IC chips are assembled into metal or dielectric substrate carriers using wire-bonding or flip-chip [6] interconnect and eventually encapsulated in plastic packages or metal housings. Due to the integration of various materials and structures in a compact, limited packaging space, unwanted substrate modes [6], cavity resonance [7], feedback, or crosstalk [8, 9] occur within the packaging module. In the previous papers [6–9], this phenomenon was well analyzed and the causes were identified and design rules or various methods for suppressing them were presented. For example, the resistivity [6] of the flip chip carrier, the resonance condition of the cavity [7], the chip mounting design rule [8], and the resistance coating of the lid [10] were investigated. Several modules [1, 2, 6, 11] have been successfully developed to reflect these attempts. However, in the case of a high-gain amplification block requiring a gain of 30 dB or more, the stability problem is caused by the feedback effect [8, 9] of the reflected signal due to structural discontinuities in the packaging. That is, the radiated signals are reflected by the surrounding structures, enter the input stage of the amplification block, and are amplified, so that the entire module oscillates. Therefore, to eliminate the oscillation of the amplification block, small and medium gain amplifier modules [2, 12, 13] are connected in series using an external WG until the required gain is satisfied. An attenuator or filter is inserted between the amplifier modules to adjust the gain or remove unwanted waves [14]. However, these methods lead to bulky and expensive mm-wave radio system due to expensive additional components.

In this work, a 40 dB high-gain amplifier module integrating the isolation WG has been demonstrated for 40 GHz radio system applications. Because of the isolation WG as well as input and output WG into the metal case of the amplifier module, a low-loss and wideband MSL-to-WG transition is designed on the 5-mil thick RT5880 substrate to interconnect the amplifier IC mounted PCB with integrated WG. The simulated and tested results of the transition have been presented. The high-gain amplifier module was fabricated and its measured performance is analyzed.

2. Metal case integrating an isolation WG for high-gain amplifier module

In general, a proactive approach to suppressing this feedback effect is to effectively isolate the two adjacent amplification stages. **Figure 1** shows the metal case inserting a 15.7 mm long isolation WG between two cavities for high-gain amplifier module applications [15]. This method allows high-gain amplification without oscillation because of good isolation between two enclosed cavities in the metal case. In the each cavity, the PCB mounting an amplifier IC is assembled. Because signals radiated due to discontinuities in the metal case or PCB assembly are confined within each cavity, the amplifier IC assembled in another cavity is protected. In this work, the MSL-to-WG transition in the isolation WG as well as an input and output WG port should be designed. The WG is based on WR22 WG, whose size is $2.84 \times 5.68 \text{ mm}^2$. Two commercial amplifier ICs [16] are used for high-gain amplification block with the gain of 40 dB. The signal line on the PCB is the 50 Ω microstrip line (MSL). Considering the inserted isolation WG and port WGs, four MSL-to-WG transitions are needed. The main key design issue is the low-loss and wide-band transition.

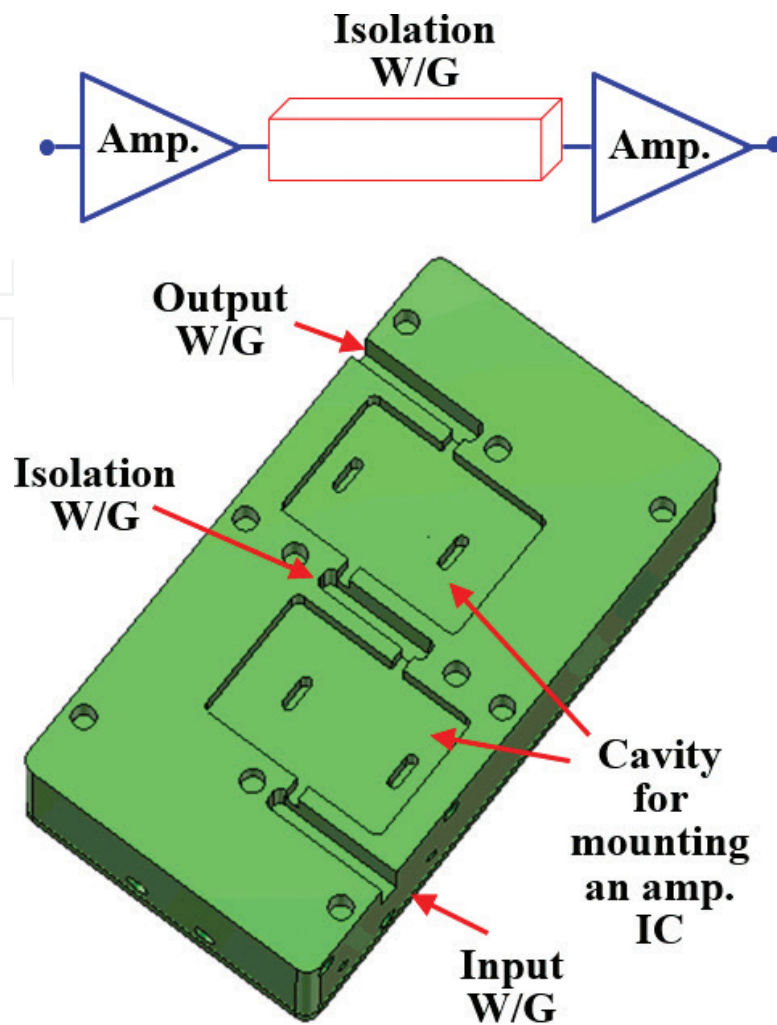


Figure 1. The metal case integrating an isolation WG for high-gain amplifier module applications.

3. Design and measurement of the low-loss and wideband MSL-to-WG transition

Figure 2 presents a configuration of the MSL probe transition, transition module for measurement, and opening in the WG side to insert the transition. For this MSL-to-WG transition, a simple electric (E)-plane transition [17, 18] is used because of easy and simple design. In this transition, a TE₁₀-mode energy in the WG couples to quasi-TEM-mode one in the MSL. The MSL transition consists of an E-plane probe, impedance transformer, and 50-Ω MSL. They are printed on a 5 mil thick substrate with a permittivity of 2.2 [19]. The size of the E-probe is $383 \times 1465 \mu\text{m}^2$. The simple high-impedance matching line with is designed for easy design and optimization. Its size is $295 \mu\text{m} \times 1000 \mu\text{m}$. The $363 \mu\text{m}$ wide MSL is designed for the 50-Ω impedance and its length between two transitions is 18.0 mm considering the cavity size in the metal case as shown in **Figure 2(b)**. A back-to-back structure is required for measurement of the fabricated MSL-to-WG transition. Two sets of the back-to-back structured transition are required to apply to the metal case as shown in **Figure 2(b)**. The E-probe of the transition is

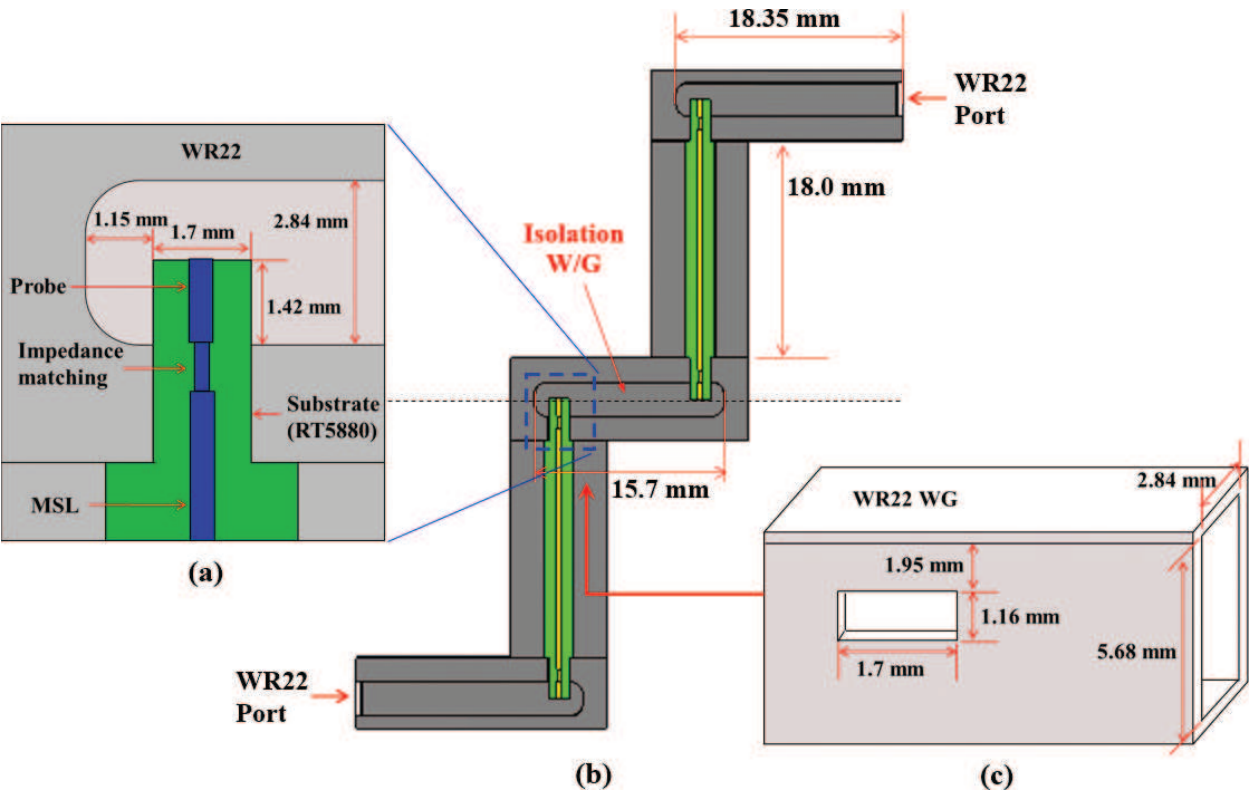


Figure 2. The configuration of the MSL probe transition (a), transition module consisting of four MSL-to-WG transitions (b), and opening in the WG side into which the transition is inserted.

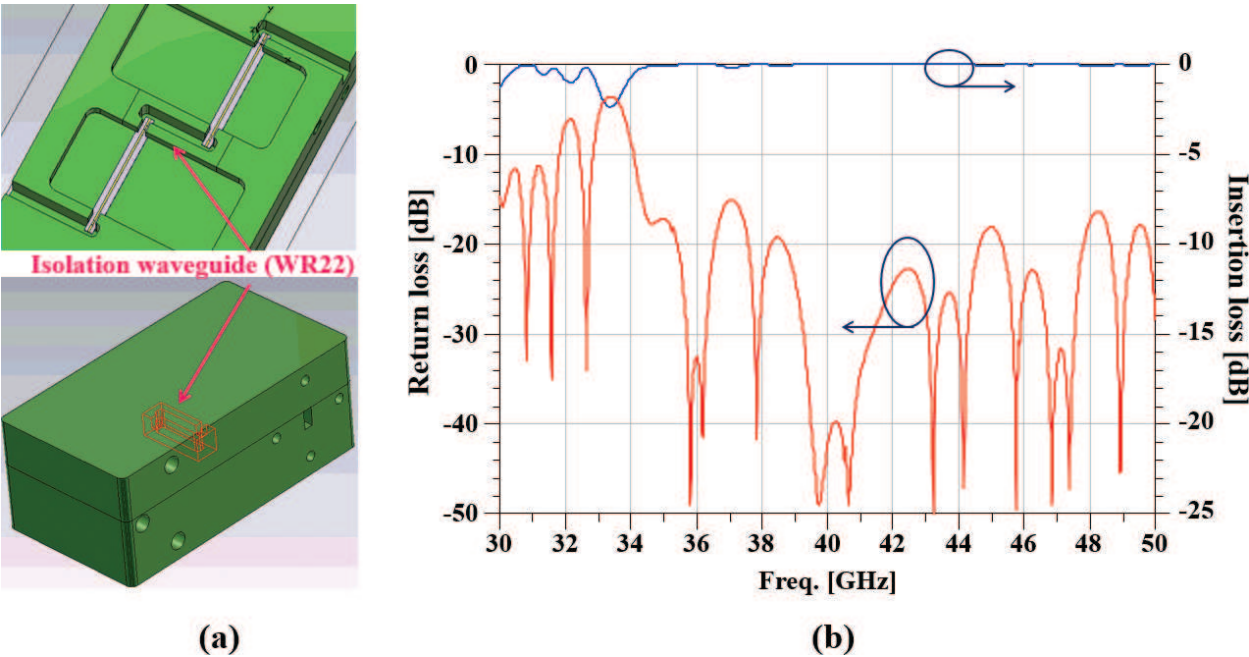


Figure 3. The metal case integrating transitions (a) and the designed results of the transition (b).

inserted into the side opening of the WG. Of course, its position and size should be optimized and the final dimensions are shown in **Figure 2(c)**.

Using electromagnetic (EM) analysis software [20], transitions were designed and analyzed. In **Figure 3**, the design model and results are presented. The transitions are designed to be assembled in the metal case. Since the WG must be integrated in the metal case, it is divided into two parts, the body and the lid. In **Figure 3(a)** and **(b)**, the metal case integrating transitions and the designed results are presented, respectively. In these designed results, an input

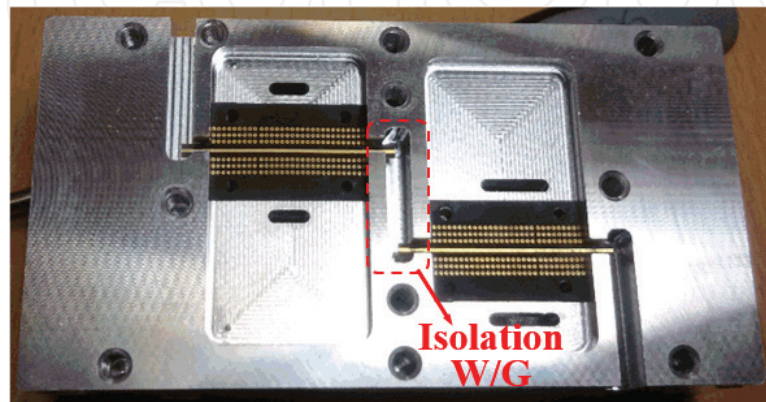


Figure 4. Fabricated transitions and assembled in the metal case.

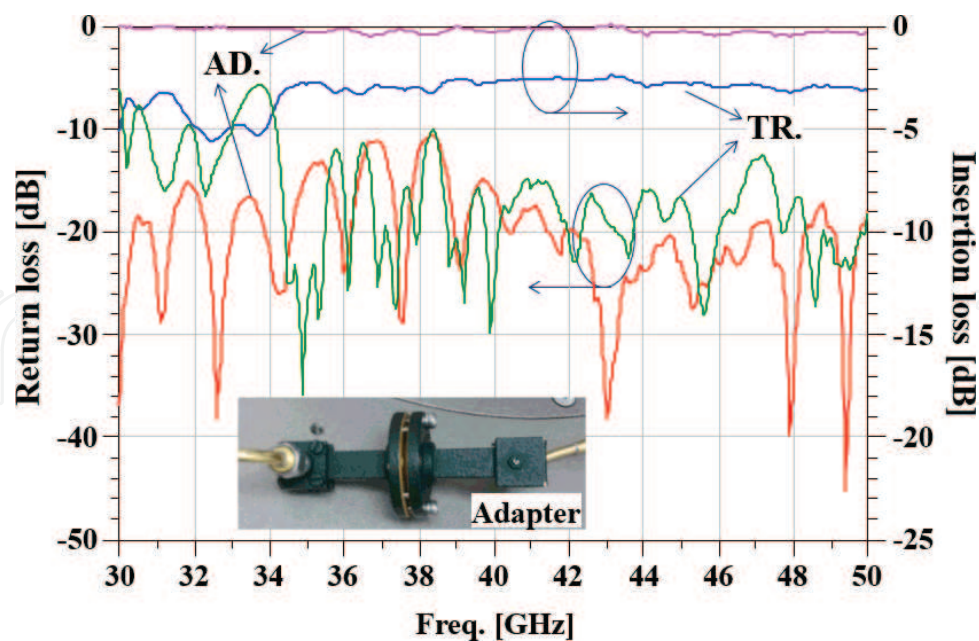


Figure 5. Measured results of the fabricated two-set transition (TR) in the back-to-back structure [an inset: an adapter connection, AD: adapters].

return loss (S11) less than -10 dB and insertion loss (S21) lower than -0.52 dB are obtained from 34.09 GHz up to 50 GHz.

The designed transitions were realized on the RT5880 substrate in commercial PCB foundry and two sets of the fabricated transitions were assembled on the metal case for the high-gain amplifier module as shown in **Figure 4**.

The measured loss characteristics of the adapters and fabricated transitions are presented as shown in **Figure 5**. Since the input and output port of the fabricated metal case is the WR22 WG, a 2.4 mm-male cable-to-WR22 WG adapters were used for connection with a vector network analyzer (VNA, Agilent N5250A) as shown in an inset of **Figure 5**. Losses of the adapters and the assembled two-set transitions were tested using the standard open-short-load (SOL) calibration from 30 to 50 GHz. The measured insertion and return loss of the adapters (AD) are from -0.26 to -0.33 dB and less than -10 dB, respectively, from 30 to 50 GHz. For the assembled two-set transitions (TR), the insertion losses of -2.9 and -2.5 dB are observed at 38 and 41 GHz, respectively. This measured insertion loss of the transition includes several loss components came from the adapters, two 18 mm long MSLs with the loss of -0.0239 dB/mm, and the MSL-to-WG transitions. By considering these loss components, the loss per a single transition is -0.32 and -0.44 dB at 38 and 41 GHz, respectively. Its measured return loss of the transition is below -10 dB from 34.1 to 50 GHz. The operational bandwidth (BW) of the transition for a return loss of -10 dB is 15.9 GHz.

4. Fabrication and measurement of the high-gain amplifier module

The high-gain amplifier module was designed and fabricated for the purpose of demonstration of the isolation WG integrated in its metal case. **Figure 6** presents PCB layout to mount

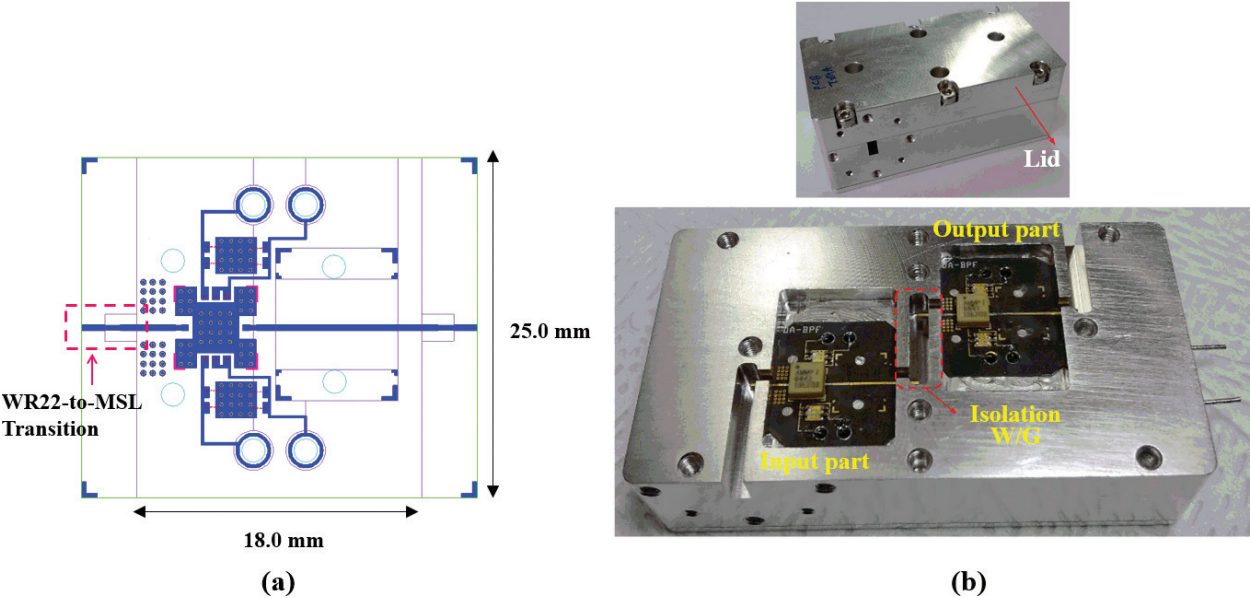


Figure 6. PCB layout to mount the amplifier IC (a) and the fabricated high-gain amplifier module (b).

the amplifier IC and the fabricated high-gain amplifier module. Landing patterns to mount a SMT-type amplifier IC [16] are designed on the RT5880 substrate by referring to application note [21] as shown in **Figure 6(a)**. In this substrate, MSL-to-WG transitions are also included to connect with WG. The designed PCB were fabricated and assembled with several components. Two PCBs were assembled in the metal case. The assembled high-gain amplifier module and the lid closed one are shown in **Figure 6(b)**. Its overall size is $79 \times 42 \times 32 \text{ mm}^3$.

The insertion and return losses of the fabricated high-gain amplifier module were measured at DC bias conditions ($V_d = 5 \text{ V}$ and $I_d = 1000 \text{ mA}$) and the measured results are presented in **Figure 7**. For comparison purposes, the characteristics plotted based on the data in a data-sheet of the single amplifier IC [16] are also shown. For the high gain amplifier module, the gain more than 39.7 dB was measured at 38–41 GHz. At 38.7 GHz, the maximum gain of 44.25 dB is obtained [15].

Considering a single amplifier IC with the gain of 20 dB, a gain of 40 dB for the high-gain amplifier module connecting two amplifier ICs in series means that the transition loss is negligible. Therefore, these results demonstrate that the isolation WG provides good isolation between two amplifier ICs and suppress effectively feedback effects in the high-gain amplification block. Compared to the return losses ($|S_{11}|$ data and $|S_{22}|$ data) of the single amplifier IC, the return loss ($|S_{22}|$ meas) at output connection part of the high-gain amplifier module is

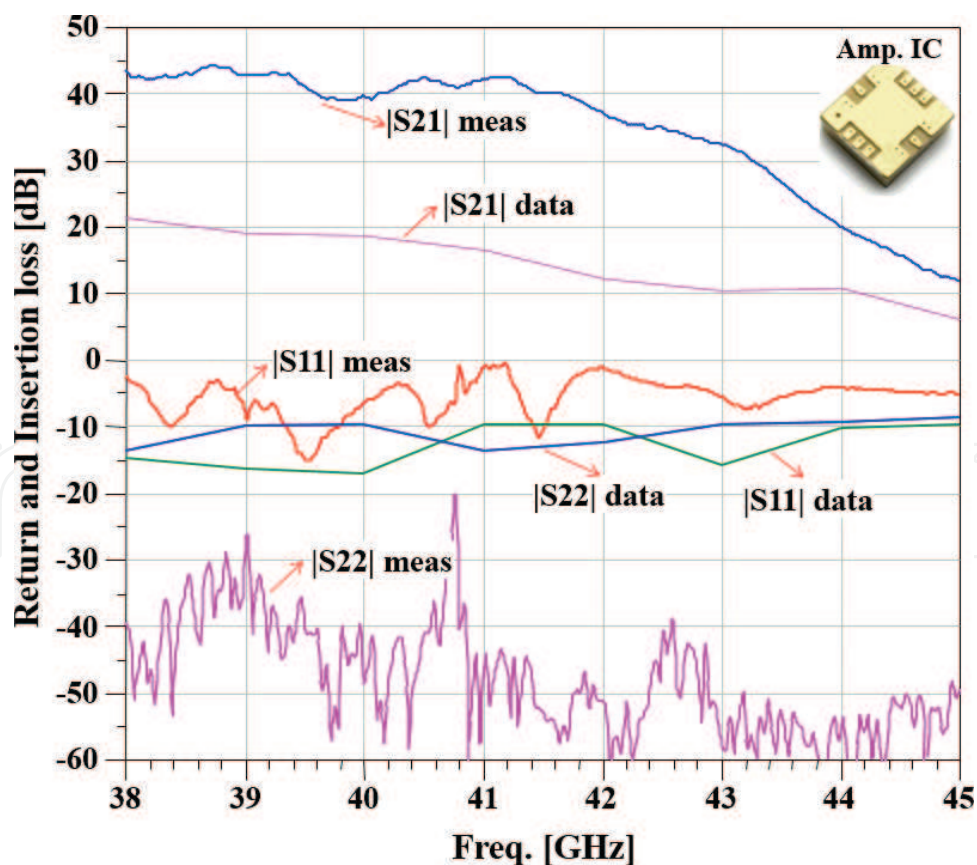


Figure 7. Measured results of the fabricated high-gain amplifier module, compared to amplifier IC (AMMP-6441) ones from its data sheet [M: measurement and amp. IC: data sheet of an amplifier IC].

noticeably improved, but the return loss ($|S_{11}|$ meas) at its input connection part is degraded. In general, the return loss of an assembled amplifier module follows the return loss characteristic of the transition. Therefore, the improvement of $|S_{22}|$ meas is due to the characteristics of the transition. However, the deterioration of $|S_{11}|$ meas at the input stage is caused by alignment and PCB fabrication process problems during assembly of the WG and PCB transitions.

5. Conclusion

The 40 dB high-gain amplifier module with the isolation waveguide (WG) has been presented for millimeter wave applications. For the purpose of suppressing the oscillation due to the feedback effect, the isolation WG was integrated into the metal case of the amplifier module. In addition to input/output WG of the amplifier module, additional MSL-to-WR22 WG transitions are required due to the isolation WG and low-loss and wide-band transition is designed and manufactured on the 5 mil thick RT5880 substrate. Its measured loss and operational bandwidth were less than -0.44 dB/a transition and 15.9 GHz, respectively at 40 GHz. The high-gain amplifier module was designed and fabricated for the purpose of demonstration of the isolation WG. The amplifier module operated stably without oscillation at high gain over 40 dB. The fabricated high-gain amplifier module showed a high gain over 39.7 dB from 38 to 41 GHz. Its maximum gain of 44.25 dB was obtained at 38.7 GHz.

Author details

Young Chul Lee

Address all correspondence to: rfleeyc@gmail.com

Division of Marine Mechatronics, Mokpo National Maritime University, Republic of Korea

References

- [1] Tessmann A, Kudzusz S, Feltgen T, Riessle M, Sklarczyk C, Haydl WH. A 94 GHz single-chip FMCW radar module for commercial sensor. In: IEEE MTT-S International Microwave Symposium. Vol. 3. 2002. pp. 1851-1854. DOI: 10.1109/MWSYM.2002.1012223
- [2] Tessmann A, Leuther A, Kuri M, Massler H, Riessle M, Essen H, Stanko H, Sommer R, Zink M, Stibal R, Reinert W, Schlechtweg M. 220 GHz low-noise amplifier modules for radiometric imaging applications. In: The 1st European Microwave Integrated Circuits Conference. 2006. pp. 137-140. DOI: 10.1109/EMICC.2006.282770
- [3] Kim J-G, Kang D-W, Min B-W, Rebeiz GM. A single-chip 36-38 GHz 4-element transmit/receive phased-array with 5-bit amplitude and phase control. In: IEEE MTT-S International Microwave Symposium. 2009. pp. 561-564. DOI: 10.1109/MWSYM.2009.5165758

- [4] Yaakob S, Samsuri NM, Mohamad R, Farid NE, Azmi IM, Hassan SMM, Khushairi N, Rahim SAEA, Rahim AIA, Rasmi A, Zamzuri AK, Idrus SM, Fan S. Live HD video transmission using 40GHz radio over fibre downlink system. In: IEEE 3rd International Conference on Photonics (ICP). 2012. pp. 246-249. DOI: 10.1109/ICP.2012.6379854
- [5] Al-Falahy N, Omar YA. Technologies for 5G networks: Challenges and opportunities. IT Professional. 2017;**19**(1):12-20. DOI: 10.1109/MITP.2017.9
- [6] Tessmann A, Riessle M, Kudzus S, Massler H. A flip-chip packaged coplanar 94 GHz amplifier module with efficient suppression of parasitic substrate effects. IEEE Microwave and Wireless Components Letters. 2004;**14**:145-147. DOI: 10.1109/LMWC.2004.827115
- [7] Dhar J, Arora RK, Dasgupta A, Rana SS. Enclosure effect on microwave power amplifier. Progress in Electromagnetics Research C. 2011;**19**:163-177
- [8] Krems T, Tessmann A, Haydl WH, Schmelz C, Heide P. Avoiding cross talk and feedback effects in packaging coplanar millimeter-wave circuits. In: IEEE MTT-S International Microwave Symposium. Vol. 2. 1998. pp. 1091-1094. DOI: 10.1109/MWSYM.1998.705183
- [9] Beilenhoff K, Heinrich W. Excitation of the parasitic parallel-plate line mode at coplanar discontinuities. In: IEEE MTT-S International Microwave Symposium. Vol. 3. 1997. pp. 1789-1792. DOI: 10.1109/MWSYM.1997.596891
- [10] Yook J-G, Katehi LPB, Simons RN, Shalkhauser KA. Experimental and theoretical study of parasitic leakage/resonance in a K/Ka-band MMIC package. IEEE Transactions on Microwave Theory and Techniques. 1996;**44**(2):403-410. DOI: 10.1109/22.554569
- [11] Lee YC, Chang W-I, Park CS. Monolithic LTCC SiP transmitter for 60GHz wireless communication terminals. In: IEEE MTT-S International Microwave Symposium. 2005. pp. 1015-1018. DOI: 10.1109/MWSYM.2005.1516839
- [12] Radisic V, Mei X, Sarkozy S, Yoshida W, Liu P-H, Uyeda J, Lai R, Deal WR. A 50 mW 220 GHz power amplifier module. In: IEEE MTT-S International Microwave Symposium. 2010. pp. 45-48. DOI: 10.1109/MWSYM.2010.5515248
- [13] Tessmann A, Leuther A, Hurm V, Massler H, Zink M, Kuri M, Riessle M, Losch R, Schlechtweg M, Ambacher O. A 300 GHz mHEMT amplifier module. In: IEEE International Conference on Indium Phosphide & Related Materials. 2009. pp. 196-199. DOI: 10.1109/ICIPRM.2009.5012477
- [14] Samoska L, Church S, Cleary K, Fung A, Gaier TC, Kangaslahti P, Voll P. Cryogenic MMIC low noise amplifiers for W-band and beyond. In: International Symposium on Space Terahertz Technology. 2011
- [15] Lee YC. Waveguide integrated high-gain amplifier module for millimeter-wave applications. Progress in Electromagnetics Research Letters. 2015;**57**:125-130
- [16] Avago Technologies. AMMP-6441 36-40 GHz, 0.4 W Power Amplifier in SMT Package [Internet]. Available from: http://www.datasheetlib.com/datasheet/168419/ammp-6441-tr2g_avago-technologies.html

- [17] Leong Y-C, Weinreb S. Full band waveguide-to-microstrip probe transitions. In: IEEE MTT-S International Microwave Symposium; 1999. pp. 1435-1438. DOI: 10.1109/MWSYM.1999.780219
- [18] Shireen R, Shi S, Prather DW. W-band microstrip-to-waveguide transition using via fences. Progress in Electromagnetics Research Letters. 2010;**16**:151-160
- [19] Rogers Corporation. Available from: <http://www.rogerscorp.com>
- [20] CST Microwave Studio. Available from: <https://www.cst.com>
- [21] Avago Technologies. Application note 5520-AMxP-XXXX Production Assembly process (Land Pattern A) [Internet]. Available from: <http://www.avagotech.com/docs/AV02-2954EN>

IntechOpen